(Abstract for the 6th International Workshop on Water Waves and Floating Bodies, April 1991)

NONLINEAR INTERACTIONS BETWEEN A FREE SURFACE AND A VORTEX SHEET SHED BY A MOVING SURFACE-PIERCING PLATE

Wu-ting Tsai and Dick K. P. Yue
Department of Ocean Engineering
MIT, Cambridge, MA 02139, USA

1. Introduction

We present preliminary results for the numerical simulation of the fully-nonlinear interactions between the vortex sheet shed by a surface-piercing moving body and the free surface above it in two-dimensional, inviscid flow. Historically, vortex dynamics studies have been applied primarily to aerodynamic and hydrodynamic problems without free surfaces. It is only in recent years that there is increasing attention on the important and fundamental problem of free surface and vortex interactions. Such phenomena have important implications to the operation of lifting surfaces such as keels or control fins near the free surface, and to the wave resistance and free-surface disturbances that may be created. To simplify the problem, we focus our attention on a body with a sharp edge for which a simple model for vortex generation can be used.

The initial-boundary-value problem for the vortex/free surface simulation is solved using a mixed-Eulerian-Lagrangian approach (*e.g.*, Longuet-Higgins & Cokelet 1976; Vinje & Brevig 1981). It is known that this approach suffers from numerical instabilities such as saw-tooth oscillations on the free surface and irregular motions of the vortex sheet, which arise from either computational errors or ill-posedness of the problem. There have been numerous efforts, such as smoothing (Longuet-Higgins & Cokelet 1976), rediscretization (Fink & Soh 1974) and regularization methods (Chorin & Bernard 1973), to modify or stabilize the numerical scheme. These stabilizing techniques in effect introduce damping into the dynamical system, or a filter which suppresses the unstable modes. A common criticism of all these techniques is that the precise relationship between the computational results and the 'exact' solution and ultimately the actual physical problem is unclear. Our view is that with the limitations of the mathematical formulation in representing the physical model, and with the complexity of the physical system itself, there is much to be gained by accurate simulation and quantification of the global features despite the (inevitable) use of stabilizing techniques. (The alternative of adopting full viscous free-surface codes is prohibitive in most cases.) We are especially encouraged by the promising results of Vinje & Brevig (1981) for simulation of nonlinear free surface motions, and by Faltinsen & Pettersen (1982) for vortex sheet tracing. The numerical procedures adopted in the present simulation are primarily generalizations and extensions of these two works.

2. Formulation

We consider as a canonical problem the abrupt starting from rest to horizontal velocity U of an infinitesimally thin vertical surface piercing strut of submergence h. The free shear layer is assumed to be confined in an infinitesimal vortex sheet. Significantly, for deep water, this problem is governed by only one parameter, the Froude number $F_n = U/\sqrt{gh}$. In the following, length and time units are chosen so that h, g=1.

The computational domain is enclosed by imposing periodic boundary conditions on the upstream ($x = \ell/2$) and downstream ($x = -\ell/2$) vertical boundaries. The contour of the domain consists of the free surface (C_f), the plate with fluid on one side (C_p), the submerged portion of plate (C_s) and the vortex sheet (C_v). Since the complex potential $\beta(z,t) = \phi + i\psi$ is analytical inside the fluid domain, Cauchy integral theorem gives for each time instant t:

$$\beta(z_k,t) = \frac{1}{i\pi} \oint_{C_f \cup C_p} \beta(z,t) K(z;z_k) dz + \frac{1}{i\pi} \int_{C_s \cup C_v} [\phi(z,t)] K(z;z_k) dz + i2\tilde{\beta}_\infty(t); \qquad (1)$$

when $z_k \in C_f$ and C_p, and

$$\beta^{\pm}(z_k,t) = \pm\frac{1}{2}[\phi(z_k,t)] + \frac{1}{i2\pi}\int_{C_f \cup C_p} \beta(z,t)K(z;z_k)dz + \frac{1}{i2\pi}\oint_{C_s \cup C_v} [\phi(z,t)]K(z;z_k)dz + i\tilde{\beta}_\infty(t); \quad (2)$$

when $z_k \in C_s$ and C_v; where $[\phi(z,t)] = \phi^+ - \phi^-$ is the potential jump across C_s and C_v, the kernel function $K(z;z_k) = (\pi/\ell)\cot[(\pi/\ell)(z-z_k)]$, and $\tilde{\beta}_\infty(t)$ is a complex constant resulting from contour integration along $z = [-\ell/2 - i\infty, \ell/2 - i\infty]$.

Taking the imaginary and real parts of (1) for $z_k \in C_f$ and C_p respectively, we obtain second-kind Fredholm integral equations for ψ on C_f and ϕ on C_p. The imaginary part of (2) when $z_k \in C_s$ gives first-kind integral equations for the potential jump $[\phi]$ on C_s. The mixed first- and second-kinds integral equations are solved by approximating the contour by piecewise-linear segments and piecewise-linear distributions of β and $[\phi]$ along the segments. For the second-kind integral equations, the collocating points z_k are on the nodes of the line segments. For the first-kind equations, z_k are placed at the midpoints of the segments. Following Lin (1984), we specify the known β at both upper $(C_f \cup C_p)$ and lower $(C_f \cup C_p \cup C_s)$ intersection points. In order to obtain two extra equations for the complex constant, $\tilde{\beta}_\infty(t)$, we also collocate at the upper intersection point and at the midpoint of the segment above the lower intersection point.

The evolution of the free surface positions ζ and potentials $\phi(\zeta,t)$ are updated by integrating in time the kinematic and dynamic free surface boundary conditions:

$$\frac{Dz}{Dt} = w^*, \quad \text{and} \quad \frac{D\phi}{Dt} = \frac{1}{2}ww^* - \frac{1}{F_n^2}\zeta, \qquad (3,4)$$

where the complex velocities $w(z,t) = d\beta(z,t)/dz$ are calculated using three-point Lagrange formulae. The velocity at the intersection points are obtained by differentiating the values of β at nodes on the plate next to the intersection points. The vortex sheet is a material surface and is convected according to

$$\frac{Dz}{Dt} = \frac{1}{2}(w^+ + w^-). \qquad (5)$$

At the tip of the plate where the vortex sheet sheds out, Bernoulli equation gives the rate of shedding of potential jump as

$$\frac{D[\phi]}{Dt} = \frac{1}{2}(w^- w^{-*} - w^+ w^{+*}), \qquad (6)$$

where the velocities $w^{\pm}$ are calculated using the values of $\beta^{\pm}$ at the midpoints of segments on the submerged plate next to the separation point. The time integrations of (3–6) are carried out by a fourth-order Runge-Kutta scheme. The initial conditions at $t = 0$ are specified with the free surface quiescent ($\phi = 0$ and $\zeta = 0$) and a starting point vortex shed out according to the similarity solution (*e.g.*, Graham, 1983).

3. Numerical implementation and results

Figures 1 and 2 show typical computational results for F_n =1.0 and 1.5. The length of the periodic domain ℓ is 4.0, and the time step for Runge-Kutta integration is 0.005.

Because of the large deformation of the free surface, we use an adaptive rediscretizing algorithm to control the maximum length of the line segments. The typical length of segments on the free surface is 0.05. We also use a three-point smoothing formula (Longuet-Higgins & Cokelet 1976) to suppress the growth of saw-tooth instabilities on the free surface. Due to the impulsive motion of the plate, the free surface on the forward side of the plate behaves like a jet (*cf.*, Lin 1984). The upper intersection point shoots up quickly and a thin film forms along the upper part of the plate.

To avoid difficulties associated with simulating a very thin film on the plate, the portion of the film with thickness less than 2% of the length of a plate segment is eliminated and a new intersection point specified. In contrast to the free surface near the upper intersection point on the forward side of the plate, the lee side of the free surface intersects the plate at a large contact angle. For $F_n = 1.5$ the lower intersection point moves downward continuously and the free surface will eventually sluice from the lower tip of the plate. For $F_n = 1.0$ the lower intersection moves downward asymptotically to a steady depth. For even lower Froude numbers, the solutions (not presented here) are again qualitatively different.

In order to resolve the initial roll-up of the vortex sheet, a new shear layer segment is shed out continuously at each time step up to $t = 1.0$. To limit the number of spiral turns in the roll-up region of the vortex sheet, the inner portion of the spiral is amalgamated into a point vortex. Application of amalgamation is found to have only negligible effects on the motions outside the outermost turn of the spiral. As time proceeds, the vortex sheet quickly rolls up into a spiral and grows in size. For the present numerical implementation, smooth roll-up of the vortex sheet can not be achieved without applying rediscretization on the vortex sheet.

The rolled-up vortex sheet continuously grows and eventually interacts strongly with the free surface, *e.g*, for $t > 1.5$ in the figures. The free surface pushes back the vortex spiral and causes a stretch of the vortex sheet between the roll-up and the separation point (in sharp contrast to the rigid free surface, F_n=0, case.) At this stage, the rate of vortex shedding decreases to a small value and the lengths of new shear layer segments shed at the separation point become very short. To avoid instabilities associated with such short vortex segments, we control the length of the segment shed at the separation point by amalgamating new segments into one until it reaches a given length (0.02 for the results shown). We also found that the vortex sheet suffers Kelvin-Helmholtz instabilities which are in fine scale compared to the global features. Following Moore (1981), we apply a smoothing formula to the position of the vortex sheet. Our computational experience shows that the five-point smoothing formula is more effective than the three-point formula in delaying the growth of the instability.

The interaction between the free surface and vortex sheet becomes stronger as they approach each other, *e.g.*, for $t = 2.0$ and 2.5 in the figures show. Our computational results show that qualitatively different classes of interactions can result depending on the Froude number. A systematic numerical study varying the Froude number is underway which should lead to a complete understanding and quantification of the underlying mechanisms.

References

Chorin, A. & Bernard, P.S. 1973 Discretization of a vortex sheet, with an example of roll-up. *J. Comp. Phys.*, **12**.

Faltinsen, O.M. & Pettersen, B. 1982 Vortex shedding around two-dimensional bodies at high Reynolds number. *Proc. 14th Symp. Naval Hydrodynamics.*

Fink, P.T. & Soh, W.K. 1978 A new approach to roll-up calculations of vortex sheets. *Proc. Roy. Soc. Lond.* A, **362**.

Graham, J.H.R. 1983 The lift on an aerofoil in starting flow. *J. Fluid Mech.* **133**.

Lin, W.M. 1984 Nonlinear motion of the free surface near a moving body. Ph.D. thesis, MIT, Department of Ocean Engineering.

Longuet-Higgins M.S. & Cokelet, E.D. 1976 The deformation of steep surface waves on water. I. A numerical method of computation. *Proc. Roy. Soc. Lond.* A. **350**.

Moore, D.W. 1981 On the point vortex method. *SIAM J. Sci. Stat. Comput.* **2**.

Vinje, T. & Brevig, P. 1981 Nonlinear two-dimensional ship motions. *The Ship Research Institute of Norway, Rep.* R-112.81.

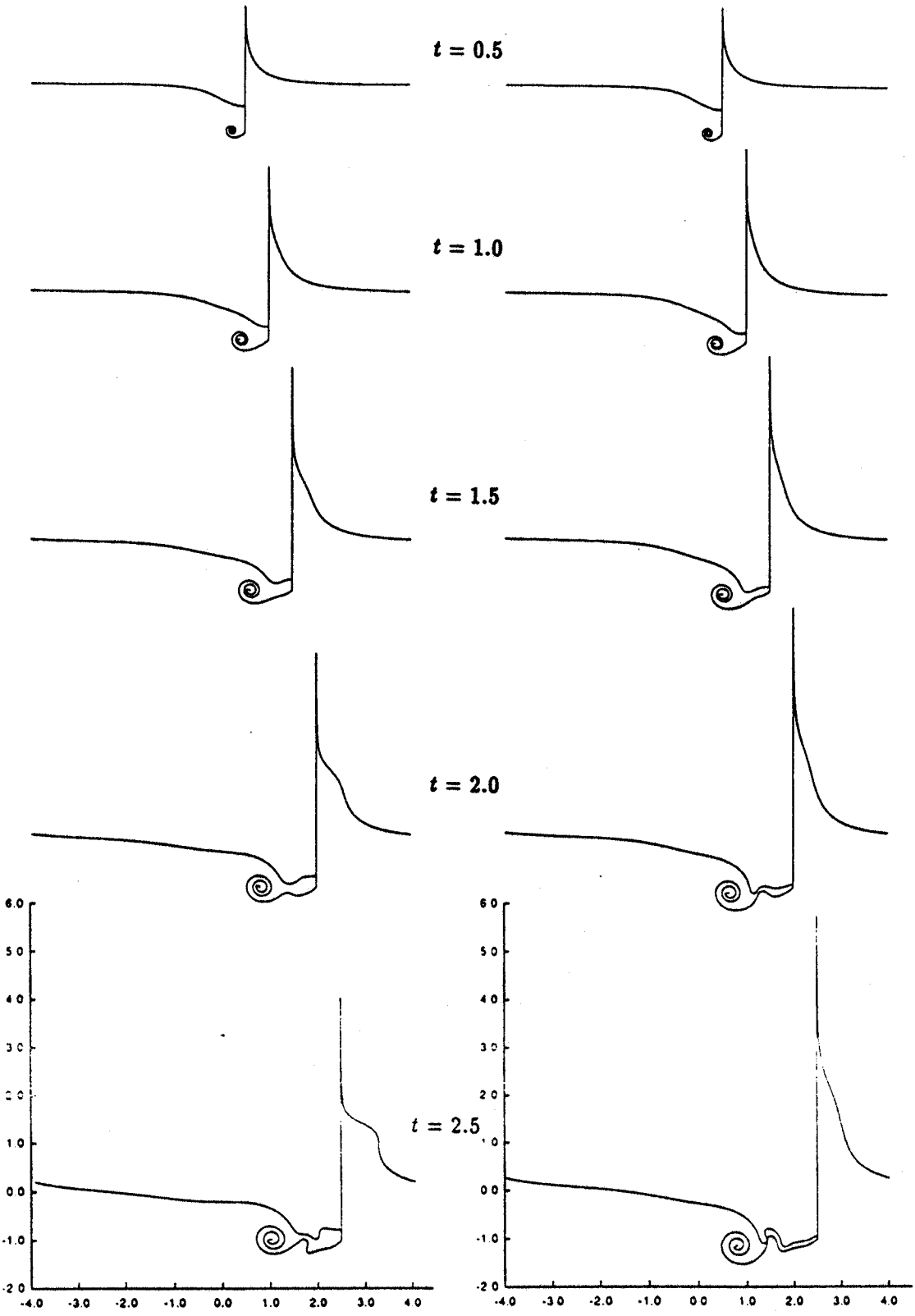

Figure 1 $F_n = 1.0$.

Figure 2 $F_n = 1.5$.

Faltinsen: In our experience, we have always thought it essential to require that the free shear layer leave the body surface tangentially. Otherwise there will, theoretically, not be any shed vorticity. In your model it does not seem to be the case that the free shear layer leaves the body surface tangentially.

Tsai & Yue: We do use Maskew's Kutta condition at the separation point and the shear layer is, in fact, shed tangentially at the tip of to the plate.

van Daalen: (1) How often do you need the adaptive rediscretization algorithm to control the maximum length of the line segments (Section 3)? (2) What is the impact of the five-point smoothing formula that you use to suppress the growth of instabilities on the free surface and do they occur on both sides of the plate? (3) Do the computations actually break down due to the thin film on the right side of the plate, and if so, can this be avoided by choosing a smaller time step?

Tsai & Yue: We rediscretize the free surface and vortex sheet at every time step for the results shown in the abstract. The regridding scheme is based on an equal-segment redistribution algorithm. We have also developed and used a new adaptive redistribution algorithm which employs a smoothing spline with curvature as the regridding mesh function. In this way, we avoid having to use the five-point smoothing formula to suppress the growth of saw-tooth instabilities. Using a small time step can only delay the thin film from moving across the plate, some form of truncation of the spray tip appears inevitable.

Clement: Would you explain why you place collocation points at the node for a 2nd kind Fredholm equation, and at the midpoints of the segments for a 1st kind equation? Did you check the condition number of the matrix to motivate this choice?

Tsai & Yue: Yes, we calculated the condition number of the coefficient matrix, and found that the matrix becomes very singular if collocation points are placed either only on nodes or only on midpoints for these mixed first- and second-kind Fredholm integral equations.